

## Chapter

# Developing a Novel Multiplexed Immune Assay Platform to Screen Kinase Modulators of T Cell Activation

*Zhaoping Liu, Andrea Gomez-Donart, Caroline Weldon, Nina Senutovitch and John O'Rourke*

## Abstract

T cell activation plays a central role in inflammation, autoimmune diseases and cancer. Cancer immunotherapies, such as immune checkpoint inhibitor, bi-specific antibody, chimeric antigen receptor T (CAR T) cell, and adoptive tumor-infiltrating lymphocyte (TIL) therapies require the characterization and monitoring of T cell activation. Here we describe a novel, multiplex immune assay platform based on high-throughput flow cytometry technology and advanced computational algorithms for data analysis. The assay simultaneously measures T cell dynamics including phenotype, time-dependent expression of activation markers, secreted effector cytokines, and proliferation. The assay screened a kinase chemogenomic library and identified 25 kinase inhibitors with distinct inhibition profiles on early (CD69) and late (CD25) activation markers and the cytokines IFN $\gamma$  and TNF $\alpha$ . We identified 5 kinase inhibitors with dissimilar effects on CD69 and CD25 expression, and a cluster of total 4 MEK1/2 inhibitors with similar activation profiles. The screening revealed 3 kinase inhibitors for PKC, IKK2, and MEK1/2 respectively, all with a phenotypic signature similar to ruxolitinib, a Jak1/2 inhibitor used to treat myelofibrosis disease. These results suggest this multiplexed assay platform, combined with a chemogenomic library screening, may be used as primary screen for phenotypic or target-based drug discovery, target identification, and potential drug repositioning.

**Keywords:** T cell activation, high-throughput screening, flow cytometry, kinase inhibitor, drug repositioning

## 1. Introduction

Unraveling the complex biochemistry of the immune system in search of innovative therapies is a new frontier of drug discovery with hundreds of autoimmune disease therapies and thousands of immuno-oncology therapies in the global development pipeline [1, 2].

Hallmarks of autoimmune disease pathogenesis are abnormal CD4 and CD8 T cell activation [3]. Genetic defects, mutations and other mechanisms resulting in increased T cell activity are involved in many autoimmune pathologies making

them attractive targets for the direct inhibition of T cell activation [4]. T helper cells—characterized by the expression of the surface molecule CD4—release cytokines that shape the immune response and pathology in autoimmune and inflammatory diseases [5].

Cancer immunotherapies are moving to the forefront of cancer treatment with a variety of regimens, such as immune checkpoint blockade therapies targeting T cells' regulatory pathways to enhance T cell activation and its anti-tumor immune responses. Focusing on immune checkpoint inhibitors is a disruptive change in immuno-oncology. Rather than directly attacking the tumor cell itself, the checkpoint inhibition strategy is removing inhibitory pathways by targeting the molecules involved in T cell regulation that block effective anti-tumor responses [6]. Another type of cancer immunotherapy consists of bispecific antibodies designed to redirect immune cells to tumor sites where they induce immune synapse formation, immune cell activation, cytokine secretion and proliferation leading to tumor lysis [7].

The versatile T cell weapon can also be deployed directly via adoptive T cell transfer (ACT). ACT involves infusion of in vitro expanded antigen-specific lymphocytes such as chimeric antigen receptor T (CAR-T) cells or tumor infiltrating lymphocytes (TILs) to cancer patients to mediate antitumor effects [8–10]. The T cell-mediated tumor cell killing is through tumor antigen recognition, robust T cell activation, proliferation and in vivo cytotoxicity. Different types of cancer immunotherapies can be combined or given sequentially to further enhance the magnitude of antitumor immune response over single agents [11].

In the adaptive immune response, the binding of the T cell receptor to peptides complexed with the major histocompatibility complex (MHC) on antigen-presenting cells, along with engagement of co-receptors such as CD4 or CD8 and co-stimulatory molecules such as CD28, triggers an intricate signal cascade. The key to T cell-mediated immune responses are the multiple intracellular biochemical events involving the complex interaction of cytosolic tyrosine kinases and serine-threonine kinases [12]. Kinases as drug targets have been investigated for decades in autoimmune disease, cancer, and degenerative diseases [13]. The kinase signaling pathway through Raf/MEK/ERK1/2 is a major regulator of cell proliferation and survival, and hyper-activation of this pathway is associated with human tumor malignancies [14]. Currently 37 kinase inhibitors have received FDA approval for treatment of malignancies such as breast and lung cancer. There are 150 kinase-targeted drugs in clinical trials, and kinase-specific inhibitors are in the preclinical stage of drug development [15]. In addition, combinations of kinase inhibitors are being explored for the treatment of cancer, and preclinical and clinical data demonstrate that therapeutic combinations enhance primary antitumor responses and delay the onset of resistance [16]. Kinase signaling also regulates the immune system and modulates the tumor immune microenvironment. Inhibition of kinase activity such as phosphoinositide 3-kinase (PI3K) promotes anti-tumor immunity through direct enhancement of CD8+ T cell activation and suppression of T regulatory cells [17]. The combination of kinase inhibition with cancer immunotherapy is another emerging research area as demonstrated in recent preclinical studies that showed the kinase inhibitor of P21 Activated Kinase 4 (PAK4) boosted PD-1 therapy in animal models [18].

Whether it is the characterization of immune phenotype or function, or the screening or profiling of biological or small molecule drug candidates, high-throughput flow cytometry and its ability to perform multi-parametric analyses of single cells or particles is playing an increasingly pivotal role in quantifying the myriad aspects of drug discovery [19, 20]. Here we developed a novel, multiplexed T cell activation assay platform based on high-throughput flow cytometry and associated advanced data analysis algorithms. As a proof-of concept, we screened a

kinase chemogenomic compound library and identified kinase inhibitors with various inhibition profiles of T cell activation, monitored by sampling a small aliquot from a mixture of cells and beads in a microtiter plate.

## 2. Materials and methods

### 2.1 Cell lines and reagents

The kinase inhibitor library (Cayman, Cat#10505) used for the screening assay has 152 known kinase inhibitors at 10 mM stock concentration in DMSO. The fluorescent antibodies against CD3, CD4, CD8, CD69, CD25 and HLA-DR, cell viability dye, cell proliferation tracing dye, cytokine capture beads (iQue QBeads®, Sartorius) and the cytokine detection reagents used in this study are from the iQue® Human T Cell Activation Kit (iQue® Sartorius, Cat#90561). Human PBMCs (Astarte Biologics, Cat#1001) from healthy donors were stimulated/activated with either T-activator CD3/CD28 Dynabeads® (ThermoFisher, Cat#11131D) or phytohemagglutinin (PHA, Sigma, Cat#L8754), or Enterotoxin Type B from *Staphylococcus aureus* (SEB, List Biological Laboratories, Cat#122). Cells were cultured in RPMI-1640 (VWR, Cat#45000–396) with 10% fetal bovine serum (VWR, Cat#97068–085) and supplements that included non-essential amino acids (VWR, Cat#12001–634), sodium pyruvate (VWR, Cat#45000–710), and penicillin–streptomycin (VWR, Cat#12001–692).

### 2.2 Assay development and characterization

#### 2.2.1 Day-to-day profiling of T cell activation

The assay was run using cryopreserved human PBMCs from a single healthy donor and were allowed to recover for 24 hours before use. On day 0, we stained human PBMCs with cell proliferation tracing dye (excitation: 488 nm and emission: 530/30 nm) and washed 3 times before plating into a 96-well plate at 2 million/mL (50 µL/well). We treated the cells by adding 50 µL/well of 3 different T-cell modulators in the respective wells: CD3/CD28 Dynabeads, PHA, or SEB. We performed an 11-point, 1:2 serial titration with duplicate wells per dose for each selected treatment. The final top concentration of the treatment in the assay well was 1 million/mL CD3/CD28 Dynabeads, 10 µg/mL PHA, or 100 ng/mL SEB, respectively. The untreated wells (with a concentration of zero) were used as negative controls for each treatment. On each day of culture (days 1, 3, and 6), we mixed the cell/supernatant sample in the culture plate by manual pipetting up and down 8 times. We transferred 10 µL cell/supernatant sample per well without dilution from the culture plate to a 96-well assay plate (Costar, Cat#3897), and stained the samples following the iQue® Human T Cell Activation Kit assay protocol. In the assay plate, 2 rows of wells (rows A and B) were designated for standard curve generation with a mixture of 2 protein standards (IFN $\gamma$  and TNF $\alpha$ ) in each well. Top concentration was 50,000 pg./mL for each protein in the standard mixture with 1:3 serial titration and duplicate wells per concentration. The lowest concentration was set to zero to determine background. Rows C–H were assigned to samples from 3 different treatment regimens: CD3/CD28 Dynabeads, PHA or SEB (**Supplemental Figure 1**). After staining and washing, samples from the full plate were acquired in approximately 15 minutes using the iQue® Screener PLUS (Sartorius), a high-throughput flow cytometry platform which has violet, blue and red lasers, and a total of 13 fluorescent channels. In each sample well of the assay plates, levels of secreted

cytokines (IFN $\gamma$  and TNF $\alpha$ ) were interpolated by reference to the corresponding standard curves generated from the standard wells in the same assay plate.

### 2.2.2 Z' factor characterization of T cell activation

The Z' factor of the assay was calculated to evaluate assay variation. The study was run similarly to the day-to-day profiling study described earlier, with minor modification. Cryopreserved human PBMCs from a single healthy donor were allowed to recover for 24 hours before use. On day 0 we plated the recovered PBMCs into a 96-well plate at 2 million/mL (50  $\mu$ L/well). Then, we treated the cells by adding the same volume of CD3/CD28 Dynabeads. Total volume per well was 100  $\mu$ L at the final concentration, with a total of 3 plates run. In each culture plate there were 24 wells without Dynabeads (negative control), and 24 treated wells with CD3/CD28 Dynabeads (positive control) with a final bead density of 1 million/mL. After culturing 24, 48, or 72-hours, we mixed the cell/supernatant samples in the culture plate by manual pipetting 8 times. We transferred 10  $\mu$ L of cell/supernatant sample per well without dilution, from the culture plates to 96-well assay plates and stained following the iQue $\text{\textcircled{R}}$  Human T Cell Activation Kit assay protocol. After staining and washing, samples from each plate were acquired on the iQue $\text{\textcircled{R}}$  Screener PLUS. iQue Forecyt $\text{\textcircled{R}}$  software was used to perform Z'-Factor plate calculations on well data of the positive and negative controls. For each plate, a single Z'-Factor was calculated as follows [Eq. 1]:

$$Z - factor = 1 - \frac{3(\sigma_p + \sigma_n)}{|\mu_p + \mu_n|} \quad (1)$$

- $\sigma_p$  = standard deviation of the positive control wells for each plate
- $\sigma_n$  = standard deviation of the negative control wells for each plate
- $\mu_p$  = mean of the positive control wells for each plate
- $\mu_n$  = mean of the negative control wells for each plate

Positive control wells: CD3/CD28 Dynabeads-treated wells with bead/cell ratio at 1:1. Both Dynabeads and PBMC concentrations were at 1 million/mL. Negative control wells: cells only without CD3/CD28 Dynabeads.

## 2.3 Kinase inhibitors screening

### 2.3.1 Culture setup for screening

The cryopreserved PBMCs from a single healthy donor were allowed to recover for 24 hours before use. On day 0 we plated the recovered PBMCs into a 96-well plate at 4 million/mL (25  $\mu$ L/well). We then added 25  $\mu$ L of 40  $\mu$ M kinase inhibitors (in culture media) into each well with cells to reach 20  $\mu$ M inhibitor concentration. The negative control was culture media only and the positive control was 20  $\mu$ M cyclosporine A. We mixed the culture and incubated for 1 hour with 5% CO $_2$  at 37 $^\circ$  C. We then added 50  $\mu$ L (2 million/mL) of CD3/CD28 Dynabeads into each well of the screening culture plate. The final cell and Dynabead density were 1 million/mL each, and the final kinase inhibitor concentration was 10  $\mu$ M. After mixing, the culture plate was incubated for 24 hours with 5% CO $_2$  at 37 $^\circ$  C.

### 2.3.2 *The screening assay*

The screening assay was performed after a 24-hour treatment. Because all wells of the 2 screening plates were filled with the kinase inhibitors and controls, we used a third plate for the standard curve generation. For the standard curve plate, only the top 2 rows were used. Top concentration for each standard in the mixture was 50,000 pg./mL, with a 1:3 serial titration and duplicate wells. The lowest concentration was zero for negative control purposes. After a 24-hour culture for the 2 screening culture plates, we mixed the cell/supernatant samples in the culture plates by manual pipetting up and down 8 times and then transferred 10  $\mu$ L of the cell/supernatant sample per well, without dilution from the 2 culture plates to the 2 screening assay plates. We stained the plates following the iQue® Human T Cell Activation Kit assay protocol. After staining and washing, the samples from each plate were acquired on the iQue® Screener PLUS. After data acquisition, the secreted levels of 2 cytokines (IFN $\gamma$  and TNF $\alpha$ ) in the 2 screening plates were interpolated using the iQue Forecyt® software by referring to the corresponding standard curves generated from the standard-only plate.

### 2.3.3 *Dosage test of kinase inhibitors*

After screening the kinase inhibitor library, we selected some compounds for further characterization by dosage testing. The test workflow was the same as the screening workflow described earlier with the exception of a series of kinase inhibitor concentrations. We performed 11-point, 1:2 serial titration with duplicate wells per dose for each selected compound. The final top concentration in the assay well was 10  $\mu$ M for each selected compound. The concentration at zero  $\mu$ M was used as negative control (background) for each compound.

### 2.3.4 *General data acquisition and analysis method*

The iQue® Human T Cell Activation Kit comes with a template with predefined gates. Other analytical functions, such as heat maps, are queued to automatically populate. During data acquisition, events populated in the dot plots within the templated gates. The iQue QBeads® (for cytokine quantitation) and the cells were segregated based on size. Singlet beads were gated in a 2D plot of forward scatter (FSC)-height vs. FSC-area. After data acquisition on the iQue® Screener PLUS, all the cell and bead populations of interest were gated at the plate level. As shown in **Figure 1B**, the gating strategy separates cytokine capture beads from PBMC cells in an FSC vs. side scatter (SSC) plot, based on size and granularity differences. Singlet beads were gated in an FSC-height vs. FSC-area, and 2 different cytokine capture beads (iQue QBeads®) were separated in an RL1 (excitation: 640 nm; emission: 675/30 nm) vs. RL2 (excitation: 640 nm; emission: 780/60 nm) plot. Singlet cells are gated in an FSC-height vs. FSC-area plot. Live cells were gated in an RL1 vs. SSC plot. In live cell population, proliferated cells (dim fluorescent population) were gated from non-proliferated cells (bright fluorescent population) by using an overlay BL1 (excitation: 488 nm; emission: 530/30 nm) 1D histogram with positive and negative controls (data not shown). Also, from the live cell population, CD3<sup>+</sup> T cells were separated from non-T cells in a CD3 vs. SSC plot. CD4<sup>+</sup> T helper cells were separated from CD8 T cytotoxic cells in a CD4 vs. CD8 plot. CD69<sup>+</sup>, CD25<sup>+</sup> and HLA-DR<sup>+</sup> CD4 or CD8 T cells were gated in the corresponding plots with the markers at x-axis and SSC at y-axis. iQue Forecyt® software generated the standard curves (IFN $\gamma$  and TNF $\alpha$ ) using a 4-parameter logistic (4PL) regression fit with  $1/Y^2$

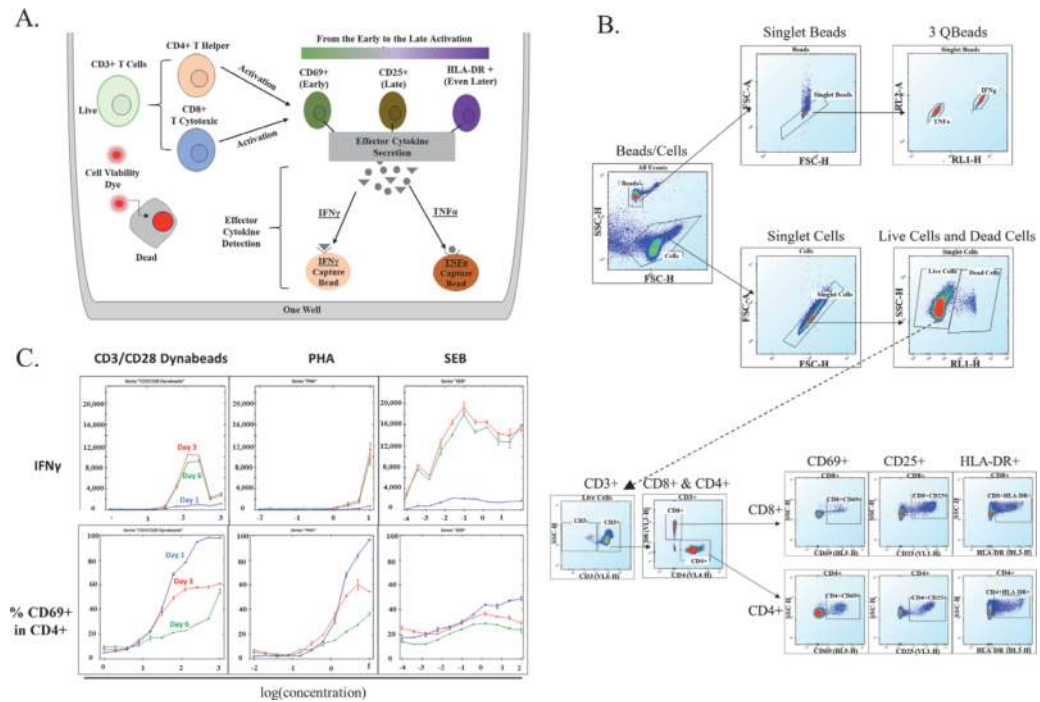


**Figure 1.** Develop a multiplexed T cell activation assay. (A) a novel multiplexed T cell activation assay in a cell and bead mixture format. T cells in each assay well are stained with cell viability dye to differentiate live cells and dead cells. Cells are stained with CD3, CD4 and CD8 fluorescent antibodies to identify the CD4+ T helper cells and CD8+ T cytotoxic cells. Different T cell activation status is analyzed by staining with cell surface markers: CD69 (early activation marker), CD25 (late activation markers), and HLA-DR (even later activation markers). In the same assay well, the secreted IFN $\gamma$  and TNF $\alpha$  after T cell activation are simultaneously measured by 2 cytokine capture beads in a sandwich immunoassay format. (B) the gating strategy for digital separation of the cytokine beads and the activated T cells acquired by high-throughput flow cytometry. After the sample from each well is acquired by iQue® screener PLUS, the cell/bead events are analyzed by iQue Forecyt® software (Sartorius), and cells and beads can be separated, based on the size and granularity, in FSC/SSC plot. IFN $\gamma$  and TNF $\alpha$  capture beads are separated, based on the different bead intrinsic fluorescence in red fluorescence channels (RL1 and RL2 with excitation both at 640 nm, and with emission 675/30 nm and 780/60 nm, respectively). For cell phenotyping gating, live cells are separated from dead cells which are brightly stained by the cell viability dye intercalated with DNA. Live cells can be separated to CD3+ T cells and CD3-non-T cells. Based on CD4 and CD8 expression level, CD4+ T helper cells and CD8+ T cytotoxic cells are separated for further identification of early activation (CD69+), late activation (CD25+) and even later activation (HLA-DR+). (C) Representative data of time dependent profiling of 3 different modulators of T cell activation assay. 3 different modulators (CD3/CD28 Dynabeads, PHA and SEB) showed distinct signature of dose-dependent and time-dependent IFN $\gamma$  secretion and the expression of early activation marker CD69. The unit is k/mL for CD3/CD28 Dynabeads,  $\mu$ g/mL for PHA, and ng/mL for SEB. Each data point represents mean  $\pm$  standard deviation ( $n = 2$  wells).

weighting factor. The linear range for each standard curve was generated automatically using iQue Forecyt® software with the following equations:

$$Y_{Bend\ Lower} = \frac{(a - d)}{\frac{(1+k)}{k}} + d \quad (2)$$

$$Y_{Bend\ Higher} = \frac{(a-d)}{(1+k)} + d \quad (3)$$

$$X_{Bend} = c \left( \frac{a - Y_{bend}}{Y_{bend} - d} \right)^{\frac{1}{b}} \quad (4)$$

- Y is the response
- X is the concentration

- a is the lower asymptote
- b is slope
- c is EC<sub>50</sub>
- d is the upper asymptote
- k is a constant equal to 4.6805

Each cytokine concentration was interpolated by reference in the iQue Forecyt® software to the corresponding cytokine standard curve generated from the same assay plate, or from the standard-only plate.

### 2.3.5 Algorithms used for hit identification

We used a multi-plate analysis algorithm in the iQue Forecyt® software and a function called Profile Map based on Boolean logic to identify hits in the screening that simultaneously met multiple specified criteria across multiple plates. The hits were also ranked and compared in a line graph.

## 3. Results

### 3.1 Assay characterization

The goal of assay characterization was to evaluate assay robustness, verify the ability to differentiate the modulators of T cell activation, and determine if the assay would require optimization to screen a chemogenomic kinase library.

The assay was designed to achieve a wide dynamic range to detect high levels of these cytokines: IFN $\gamma$ , linear range 91–22,204 pg./mL and TNF $\alpha$ , linear range 181–50,000 pg./mL. The detection range is even wider than the linear range (data not shown). This wide dynamic range ensures the detection of high levels of secreted IFN $\gamma$  and TNF $\alpha$  after T cell activation and eliminates a sample dilution step.

The assay variation was characterized and analyzed by measuring the Z' factor of 24-hour T cell activation with CD3/CD28 Dynabeads as a positive control and with untreated sample as a negative control. The mean Z' factor is 0.8 for both the percentage of CD69+ cells in CD4+ cells and for the percentage of CD69+ in CD8+ cells; 0.9 for both the percentage of CD25+ in CD4+ and for the percentage of CD25+ in CD8+ cells; –0.1 and 0.2 for the percentage of HLA-DR+ in CD4+ and CD8+ cells, respectively; 0.4 (IFN $\gamma$ ), and 0.7 (TNF $\alpha$ ). As expected, a very low Z' factor for HLA-DR endpoint is a result of the late expression of this molecule after T cell activation. Forty-eight-hour and 72-hour activation did achieve higher HLA-DR Z' factor (0.3–0.5) than 24-hour activation. Different T cell activation timing may impact the signal of each endpoint and then, correspondingly, change the Z' factors. The Z' factors of 0.5 or higher in a multiplexed cell/bead-based mixture assay, suggest that the assay variation is appropriate for screening.

In order to evaluate the assay robustness in differentiating various compounds over different treatment time, we ran a day-to-day test monitoring of T cell activation. **Figure 1** shows the assay biochemistry (**Figure 1A**), and the cell/beads gating strategy (**Figure 1B**). **Figure 1C** of the day-to-day profiling results with 3 modulators demonstrated the assay robustness as a proof of concept. Only IFN $\gamma$  and CD69+ cell endpoints are shown as examples. The results showed the 3 different

modulators had distinct profiles in IFN $\gamma$  secretion, and in the expression of the early activation marker CD69. In addition, the results displayed a day-to-day effect. For the CD3/CD28 Dynabeads-treated condition, day 1 showed a dose-dependent IFN $\gamma$  secretion, and day 3 and day 6 showed similar IFN $\gamma$  secretion and saturation at a relatively high concentration. Even more interesting, the top 2 doses on day 3 and day 6 showed reduced IFN $\gamma$  secretion (“hook” effect), which was consistent with the T cell exhaustion phenomenon characteristic of T cell activation [21]. Other endpoints also achieved distinct profiles including T cell proliferation determined by using a proliferation dye (data not shown).

### 3.2 General screening results

As shown in **Supplement Figure 1**, screening the kinase inhibitor library (Cayman 152 kinase inhibitors) involved two assay screening plates.

Screening results of the kinase inhibitors on CD69 expression are shown in **Figure 2**, an iQue Forecyt® visualization function that displays a thumbnail dot plot of each well on the plate. This example shows a CD69 vs. SSC 2D plot. The figure shows only the first screening plate with CD4 $^+$  T cells as an example. Wells highlighted in bright red boxes, as examples in **Figure 2A**, show various inhibition of CD69 expression by inhibitors of 5 different kinase classes. **Figure 2B** shows a

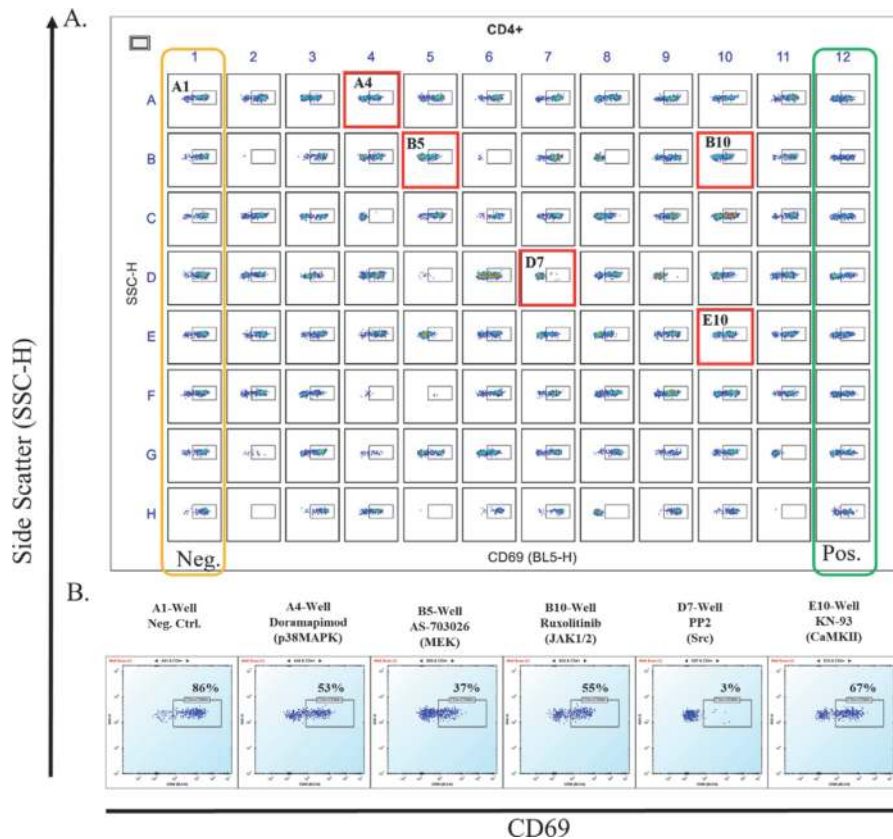


**Figure 2.**

*The representative screening results: Kinase inhibitors decrease the expression of the early activation marker CD69 on CD4 $^+$  T helper cells in the plate 1. (A) the plate view of 2D plots (CD69 vs. SSC) that showed the CD69 expression in each well. Five screening wells with decreasing CD69 expression, as examples, were highlighted with red boxes. (B) the well-based 2D plots (CD69 vs. SSC) from five highlighted wells and a negative control well (A1 well) showed different decrease of early activation marker CD69 induced by different kinase inhibitors.*



zoomed-in view of each well highlighted in red and a negative control well (A1). The results suggest the assay can pick out different compounds as hits from different classes of kinase inhibitors.

To identify hits from the screen that meet multiple criteria, we used the iQue Forecyt® multi-plate and Profile Map algorithms to distinguish hits by dialing in the exact characteristics from multiple criteria. **Figure 3A** shows the 11 thresholds used to identify hits that decrease the cytokine secretion and the expression of these cell surface activation markers: IFN $\gamma$  concentration, TNF $\alpha$  concentration, cell viability (Live Cells as % of total cells), CD4+ CD69+ as % of CD4+, CD8 + CD69+ as % of CD8+, CD4+ CD25+ as % of CD4, CD8+ CD25+ as % of CD8, CD4+ HLA-DR+ as % of CD4+, CD8+ HLA-DR+ as % of CD8+, Count of CD4+, Count of CD8+. HLA-DR was not critical in the criteria mix because it is a very late activation marker and is not highly expressed after 24 hours of activation. **Figure 3B** shows the wells (in blue) that meet the criteria specified in the iQue Forecyt® Profile Map. The positive control (cyclosporine A) is excluded from analysis (**Figure 3B**, column 12 on both plates) so that hits from only the samples can be generated for hit ranking (**Figure 3C**). The ranking is based on % CD69+ in CD4+ (from low to high). The IFN $\gamma$  and TNF $\alpha$  level was normalized against the negative control as expressed at percentage (to fit into the same scale). A total of 25 hits showed broad inhibition of all major T cell activation markers including CD69, CD25, IFN $\gamma$ , and TNF $\alpha$ . Interestingly, some patterns showed strong inhibition of cytokine secretion

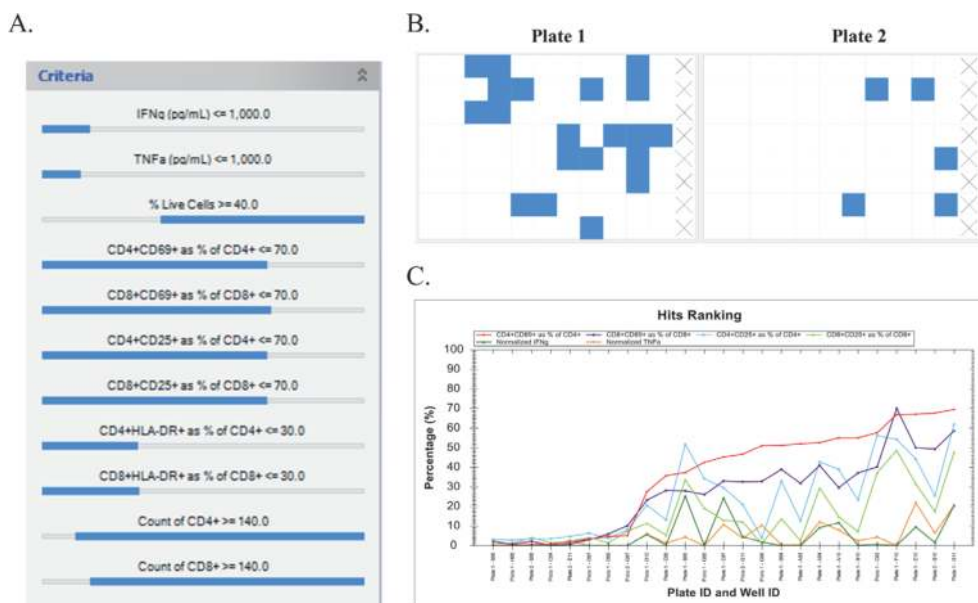


**Figure 3.** The identification and ranking of the screening hits that inhibit broadly the secreted cytokine and the expression of the cell surface activation markers. Data were analyzed by iQue Forecyt® software's multi-plate analysis and profile map tools (Sartorius). (A) the 11 criteria used to identify the screening hits. All 11 criteria were applied simultaneously to help identify the screening hits. The criteria are subjective, based on these general concepts: Inhibition of T cell activation will decrease cytokine secretion and expression of cell surface activation markers; the "hit well" should have a pre-determined number of viable T cells; and, the desired percentage of hits. (B) the profile maps of two screening plates with a total of 25 screening hits (see blue boxes). The negative control, column 1 on both plates did not show hits as expected. Column 12 (positive controls) on both plates, which did show as positive (data not shown), were excluded from analysis for the hit ranking purpose. (C) the 25 screening hits out 152 kinase inhibitors from the whole library were ranked, based on the decrease (from low to high) of CD69 expression on CD4+ T cells (red curve) by using line graph feature in iQue Forecyt®. Other parameters were also shown for the 25 hits, including CD69 expression in CD8+ T cytotoxic cells, CD25 expression in CD4+ T helper and in CD8+ T cytotoxic cells, the normalized secretion of IFN $\gamma$  and TNF $\alpha$  (normalized to the mean value of the negative wells, as expressed by the percentage).

but medium inhibition of cell surface activation markers, while some compounds strongly inhibit almost every activation marker.

### 3.3 Identification of compounds with distinct activation profiles

Using the multi-plate analysis algorithm and Profile Map Boolean logic algorithm in the iQue Forecyt® software we identified 2 compounds, tunicamycin and an erbastatin analog, that have no, or very moderate, effect on CD69+ while having medium to strong inhibition on CD25 and IFN $\gamma$  and TNF $\alpha$  (**Figure 4**). Tunicamycin

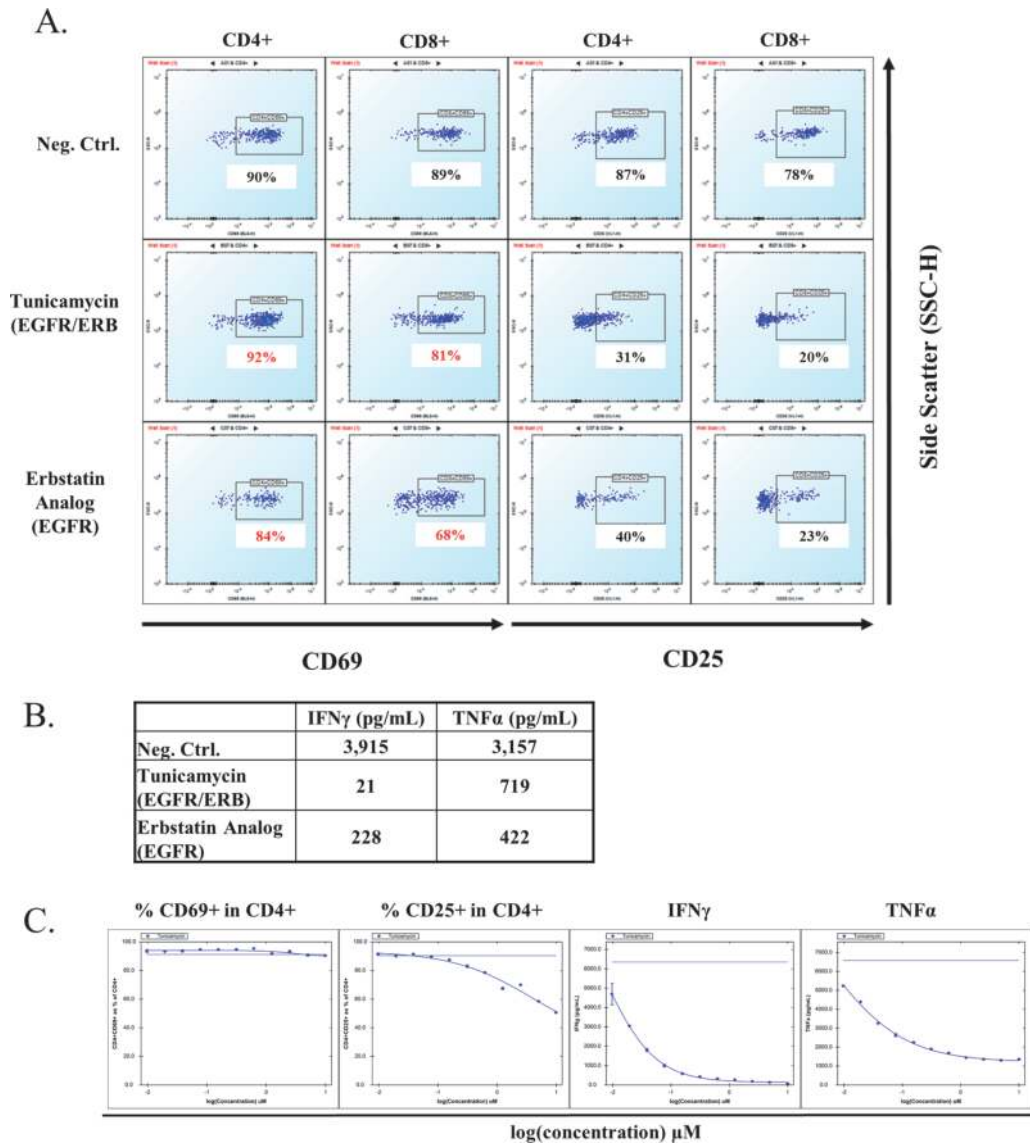


**Figure 4.** Kinase inhibitors that barely decreased early activation marker CD69 but did inhibit the expression of the late activation marker CD25 and did decrease the secreted IFN $\gamma$  and TNF $\alpha$ . (A) 2D plots (CD69 or CD25 vs. SSC) from the screening wells of these 2 inhibitors and the negative control well showed less effect on CD69 expression (see the red numbers) but with drastic decreasing effect on CD25 expression on both CD4+ T helper cells and CD8+ T cytotoxic cells. (B) Table showing the compounds Tunicamycin (EGFR/ERB inhibitor) and an erbastatin analog (EGFR inhibitor) had the significant decreasing effect on the secretion of IFN $\gamma$  and TNF $\alpha$ . (C) Example of tunicamycin's effect, from a separate dosage test experiment, on the decreasing of other markers except CD69 expression. Each point in the graph represent the mean  $\pm$  standard deviation of the duplicate wells. The dash line in each graph shows the baseline level without the compound.

decreases CD69<sup>+</sup> cells in CD4<sup>+</sup> and CD8<sup>+</sup> cells –2% and 8%, respectively, but significantly decreases CD25<sup>+</sup> cells in CD4<sup>+</sup> and CD8<sup>+</sup> cells 56% and 58%, respectively. The erbastatin analog decreases CD69<sup>+</sup> cells in CD4<sup>+</sup> and CD8<sup>+</sup> cells 6% and 21%, respectively, but significantly decreases CD25<sup>+</sup> cells in CD4<sup>+</sup> cells and CD8<sup>+</sup> cells 47% and 55%. To further confirm this effect, tunicamycin was run in a dosage test and was confirmed that it did not affect CD69 (**Figure 4C**) but inhibited other endpoints in a dose-dependent manner including CD25 expression, and the secretion of IFN $\gamma$  and TNF $\alpha$ .

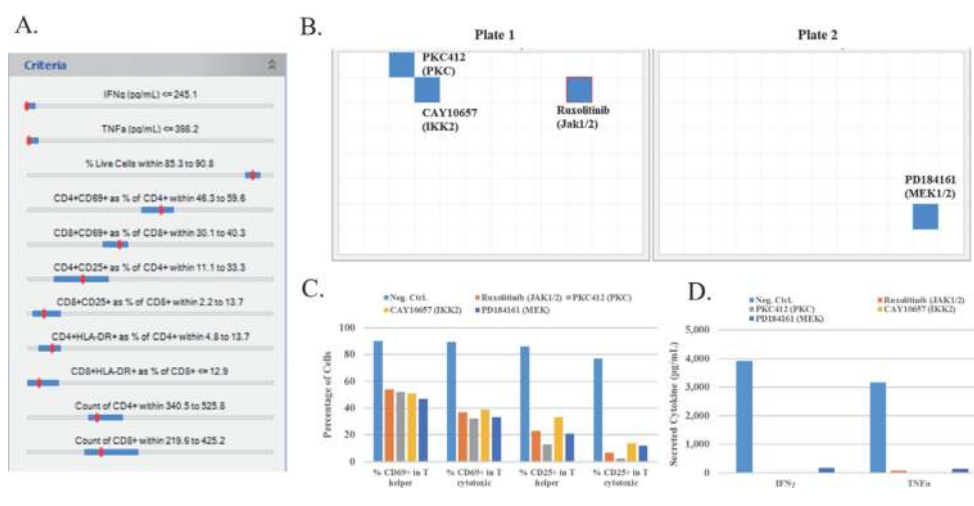
Using a similar strategy to modify different thresholds in the multi-plate visualization, we also identified the following 3 distinct kinase inhibitors that have no or very moderate inhibition effect on CD25 expression but more inhibitory effect on all other markers including CD69 and IFN $\gamma$  and TNF $\alpha$  (data not shown: U0126 (MEK1/2 inhibitor), CAY10621 (SPHK1 inhibitor), and bisindolylmaleimide V (S6K inhibitor)). Collectively, these results suggest two potential unique kinase pathways with different spatiotemporal regulation of the early activation markers CD69, and the late activation marker CD25.

### 3.3.1 Identification of a cluster of MEK1/2 inhibitors with similar activation profiles

Of the 152 kinase inhibitors in the library, there were only 4 MEK1/2 inhibitors. The screening results showed that all 4 compounds broadly inhibit the major relevant markers (CD69 and CD25 expression, and IFN $\gamma$  and TNF $\alpha$  secretion) after 24-hour T cell activation. The exception was U0126, which had less inhibitory effect on CD25 expression (**Supplemental Figure 2**). **Supplemental Figure 2A** represents the inhibitory effect of MEK1/2 inhibitors on the expression of CD69 and CD25 on both T helper and T cytotoxic cells. **Supplemental Figure 2B** illustrates the decreasing effects on the secretion of the cytokines IFN $\gamma$  and TNF $\alpha$ . In the subsequent dosage test to confirm the screening results (**Supplement Figure 2C**), 24 IC<sub>50</sub>s were generated from 4 compounds and 6 endpoints. Two MEK1/2 inhibitors AS703026 and PD0325901 showed strong potency in the inhibition of T cell activation across all 6 major endpoints. All 12 IC<sub>50</sub>s were less than 0.02  $\mu$ M. Two MEK1/2 inhibitors, U0126 and PD184161, showed moderate inhibition. A total of 11 IC<sub>50</sub>s from the latter 2 compounds were greater than 0.3  $\mu$ M. The exception was PD184161/TNF $\alpha$  with an IC<sub>50</sub> of 0.072  $\mu$ M. Although PD184161 had IC<sub>50</sub>s greater than 10  $\mu$ M for CD25 expression on T helper and T cytotoxic cells, it does inhibit CD25 expression at the highest tested dose of 10  $\mu$ M (the dosage curve not shown), similar to the performance in the screening as shown in **Supplement Figure 2A** (see the dark blue columns). High IC<sub>50</sub>s (greater than the tested highest concentration 10  $\mu$ M) were due to the lack of the bottom plateau even at the highest dose in the curve fitting.

### 3.3.2 Identification of 3 distinct kinase inhibitors with similar profiles as a well-known Jak1/2 inhibitor

One commercially valuable compound in the library, ruxolitinib, a myelofibrosis Janus kinase inhibitor with selectivity for subtypes Jak1 and Jak2, is a drug to treat disease. Ruxolitinib was shown as a positive hit in the screening. We used the iQue Forecyt® Profile Map to explore compounds similar to ruxolitinib. In the Profile Map, highlighting the ruxolitinib well triggers the algorithm to place a red tick mark in the slider bars to show the value for each endpoint of the ruxolitinib treatment (**Figure 5A and B**). By dragging and minimizing the blue slider bars for each threshold around the red mark (ruxolitinib's position), we identified 3 distinct kinase inhibitors that have profiles similar to ruxolitinib: PKC inhibitor PKC412,

**Figure 5.**

Identification of a cluster of 3 kinase inhibitors with similar phenotypic signatures as a well-known myelofibrosis drug ruxolitinib (Jak1/2 inhibitor). (A) the 11 criteria that were applied to narrow down the hits that had similar phenotypic signature as ruxolitinib. The B10 well (ruxolitinib) in plate 1 was highlighted in the profile map in iQue Forecyt® software and a red dot corresponding to the B10 wells was highlighted automatically in each threshold Bar by the profile map algorithm. By manually dragging the threshold bar from both the left end and the right end to the red dot (ruxolitinib), compounds with similar profile as ruxolitinib can be identified. Please note, these thresholds can be modified, to get more or fewer hits, according to the user's preference. (B) 3 compounds were identified from 2 screening plates with similar phenotypic signature as ruxolitinib by using the thresholds as seen in the criteria panel (A). (C) Bar graph showing the similar decreasing effect of 3 kinase inhibitors on the cell surface activation markers (CD69 and CD25) in the screening. (D) the bar graph showed the similar strong decreasing effect of 3 kinase inhibitors on the secreted cytokines (IFN $\gamma$  and TNF $\alpha$ ) in the screening.

IKK2 inhibitor CAY10657, and MEK1/2 inhibitor PD184161. It is possible to select a larger or smaller set of compounds with profiles similar to ruxolitinib by choosing a different threshold range for each endpoint. The further quantitative screening results (**Figure 5C and D**) suggest these 3 inhibitors, as similar as ruxolitinib, broadly inhibit the T cell activation markers including the expression of CD69 and CD25, and the secretion of cytokine IFN $\gamma$  and TNF $\alpha$ .

#### 4. Discussion

We developed a novel, immune assay platform that multiplexes cell and bead measurements in the same assay well. The assay analyzes T cell activation from different angles including cell health, time-dependent expression of early activation marker CD69, late activation marker CD25, even later activation marker HLA-DR, and the effector cytokines IFN $\gamma$  and TNF $\alpha$ . It is also technically possible to multiplex the measurement of other relevant cytokines in T cell activation such as IL-6, IL-10, and IL-17A, depending on biological relevance. Measuring T cell proliferation in the same assay cells involves staining with a cell tracing fluorescent dye prior to assaying. Based on the decrease of fluorescent intensity with each cell division, T cell proliferation can be simultaneously measured.

T cell activation plays a critical role in T cell-mediated tumor cell killing in cancer immunotherapy. This assay could be adapted to measure T cell activation and tumor cell killing simultaneously by barcoding target cells with a cell tracing dye prior to co-culture. A similar assay with CAR-T and tumor cell co-culture was recently reported [22].

Monitoring the condition of T cell activation during the T cell bio-manufacturing process is critical to the success of adoptive T cell therapy. As demonstrated in the results (**Figure 1**), this assay may be used for the daily monitoring of T cell activation, and to acquire time-sensitive activation information by checking simultaneously the early or late activation CD markers as well as the major effector cytokine secretion such as IFN $\gamma$  and TNF $\alpha$ . As a functional assay, it may also be used for profiling neoantigens, vaccines and other drug candidates such as immune checkpoint inhibitors, bi-specific antibodies, as well as inhibitors against inflammation or autoimmune diseases (**Figure 6**).

Using high throughput flow cytometry, this immune assay may be well-suited to the drug screening environment as we demonstrated in the Z' factor characterization. For a proof of concept, we ran a small screening campaign of a chemogenomic kinase library with 152 kinase inhibitors (each with a known target kinase protein). An iQue Forecyt® Profile Map revealed 25 of the total 152 compounds were identified as hits that broadly inhibited the T cell activation parameters, including the early activation marker CD69, the late activation marker CD25, and secreted cytokines IFN $\gamma$  and TNF $\alpha$ . Furthermore, the first 7 compounds (**Figure 3C**) showed significant inhibition of all parameters (more than 90%, compared with negative control), which suggest an upstream signal pathway simultaneously regulating the expression of all major activation markers such as CD69 and CD25 and the secretion of cytokines IFN $\gamma$  and TNF $\alpha$ .

However, it might still be an advantage to include both CD69 and CD25 in the same assay for complete insight into the cell activation. As our results suggest, CD69 and CD25 may be decoupled in the downstream signal pathway. This is supported by the finding that 2 compounds from the library screening only inhibit the expression of the late activation marker CD25, but not the early activation marker CD69 (**Figure 4**). This finding is also supported by a similar kinase inhibitor study describing new modulators of T cell receptor signaling and T cell activation [23]. In addition, we found 3 distinct kinase inhibitors that inhibited the early expression marker CD69, but not the late activation marker CD25, which further supports a theory that expression of CD69 and CD25 are regulated differently in downstream

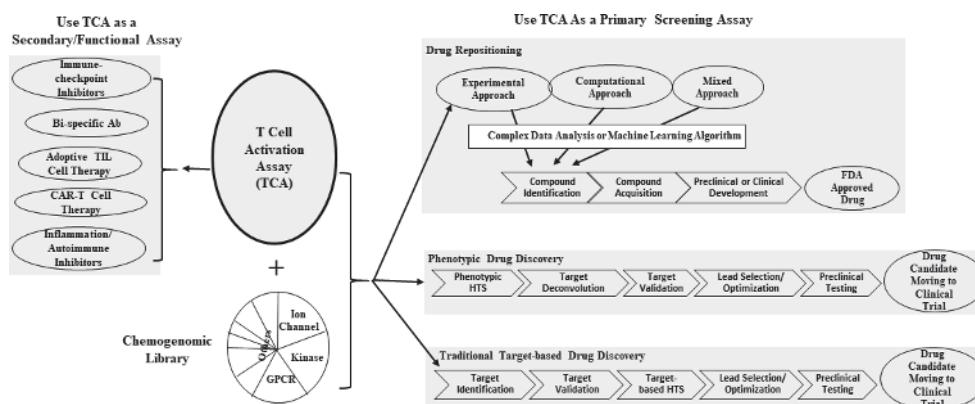


**Figure 6.** The potential screening and profiling positions of iQue® human T cell activation kit (TCA assay) in the immune drug discovery workflow. TCA assay may be used as secondary/functional assay to profile the drugs including immune-checkpoint inhibitors, bi-specific antibodies, adoptive TIL cells, CAR-T cells, and inflammation/autoimmune inhibitors. The TCA assay, together with the screening of a chemogenomic library, may be used as primary screening assay for drug repositioning, phenotypic drug discovery and traditional target-based drug discovery.

pathways. In addition, the secretion of the functional cytokines IFN $\gamma$  and TNF $\alpha$  may not share the same downstream pathway because we identified 2 different compounds (AG17, an EGFR inhibitor and Indirubin-3'-monoxime, a GSK3 $\beta$  inhibitor) that differentially decreased the secretion of one cytokine more drastically than the other (data not shown). Because 24-hour T cell activation was used as a biology model, it was not critical to analyze HLA-DR as an even later activation marker. This marker may be still useful in monitoring T cell activation for a longer term such as 5 to 10 days. The full analysis of different time-sensitive cell surface markers and the secreted cytokines may provide better insight of the precise T cell activation condition.

Of interest were several classes of compounds identified from the library that suggested drug target potential. A cluster of all four MEK1/2 inhibitors from the library showed a similar inhibition profile (**Supplement Figure 2**). In addition, 4 p38MAPK inhibitors, 3 Src kinase inhibitors, and 3 CaMKII inhibitors also showed similar inhibition profiles within each kinase inhibitor family (data not shown). These data suggest that the T cell activation assay, combined with a chemogenomic library screening, has the potential to identify possible drug targets for immune therapy.

In the kinase library screen, a blockbuster kinase inhibitor drug, ruxolitinib (Jak1/2 inhibitor, a myelofibrosis treatment), showed up as a positive hit. By adjusting the hit identification criteria in the iQue Forecyt $\text{\textcircled{R}}$  Profile Map algorithm, we identified three distinct inhibitors against three different kinase classes. These compounds showed a very similar T cell activation inhibition profile to ruxolitinib. The selection of criteria in the iQue Forecyt $\text{\textcircled{R}}$  Profile Map algorithm is subjective. It is possible that choosing a different threshold range for each criterion may result in a larger or smaller set of compounds that have inhibition profiles similar to ruxolitinib. In addition, it may be necessary to run in vitro and in vivo validation tests to further confirm the screening results. This small, proof-of-concept screening campaign showed that the multiplexed immune assay, integrated with a sophisticated data analysis algorithms, may help identify compounds or lesser-known existing drugs similar to a well-known drug. This capability may also provide potential new opportunities for kinase drug repositioning, as protein kinases are major oncology drug targets [24].

Aside from drug repositioning, there exists a need to uncover T cell activation biology as it relates to emerging immune-oncology therapies. While immune checkpoint inhibitors such as PD-1 have shown to be effective in mounting an anti-tumor response for both hematologic and solid tumors, there are further mechanistic details related to T cell activation to be learned. For example, a more complete understanding of the interactions between T cell receptors and ligands, upstream of T cell activation, and the modulation of immune checkpoint inhibition, would further progress the immuno-oncology field [25]. Unfortunately, checkpoint inhibitor therapy can result in tumor resistance, due to changes within the tumor cells and/or host immune response [26]. An option to mitigate checkpoint inhibition resistance is to enhance checkpoint inhibition with robust T cell activation via kinase inhibition [27]. Further advances in uncovering T cell activation dynamics as they relate to checkpoint inhibition therapy may include a more complete understanding of how an individual's microbiome might influence cancer treatment. Specifically, the interplay between microbiome diversity, microbiome metabolic signatures, the alteration of T cell activation and the efficacy of checkpoint inhibition therapy has been documented [25].

Both opportunities and challenges exist in phenotypic drug discovery. The small, proof-of-concept screening model described here may be extended to screen other chemogenomic libraries, such as ion channel/GPCR inhibitor, for possible target identification (**Figure 6**), or it may be extended to screen FDA-approved drug libraries for potential drug repositioning purposes. The drug candidates from the screening, particularly against immunological or immuno-oncology targets, can be further profiled by using this immune assay platform or a modified format. With all the characteristics of a functional assay, this assay platform may also be adapted for these applications: neoantigen or vaccine profiling; functional profiling of checkpoint inhibitor and bispecific antibodies in T cell activation and immune cell-mediated tumor cell killing; and daily monitoring T cell activation in the bio-manufacturing of the CAR-T and TIL cells used in adoptive T cell therapy.

## 5. Conclusions

The ability to readily characterize CD4<sup>+</sup> and CD8<sup>+</sup> T cell activation state and cytokine secretion is critical for implementing and expanding treatments for cancer, as well as autoimmune and inflammatory conditions. Protein kinase inhibition is an established strategy in oncology treatment, but additional insights are required to expand the portfolio of potential interventions. Key to these efforts is the ability to rapidly and simultaneously monitor cytokines and the temporal expression of T cell activation markers.

This work describes a multiplexed assay screen for protein kinase inhibition to identify compounds that alter T cell activation dynamics. A library of 152 chemogenomic kinase inhibitors was incubated with activated human T cells to determine the expression changes to both early (CD69) and late (CD25) T cell activation markers in conjunction with the cytokine secretion profiles for IFN $\gamma$  and TNF $\alpha$  from a single assay well. High-throughput flow cytometry screen harnessing integrated, advanced data analytics determined several inhibitors of MEK 1/2 and Jak 1/2 pathways. The existing oncology drug ruxolitinib was identified in the screen and those screen parameters were used to identify 3 additional kinase inhibitors. Importantly, the 3 kinase inhibitor screen hits alter 3 distinct kinase pathways, indicating that this approach is unlikely to show bias for a particular class of kinase activation pathway(s).

## 6. Future perspectives

Aside from the far-reaching role of T cell activation in cancer treatment, the COVID-19 pandemic has fueled the need for further research of T cell activation dynamics. There is an unmet need to better understand and identify T cell activation related to COVID-19 infection in order to improve COVID-19 treatment [28]. The extent of T cell activation in COVID-19 is associated with either recovery from infection or poor disease prognosis, such as in the cases of severe COVID-19. Interestingly, there is evidence that the enhanced expression of the late stage T cell activation marker HLA-DR is associated with severe COVID-19 [29]. Thus, the ability to perform drug treatment screens, similar to the approach described in this work, and identifying the modulation of T cell activation while simultaneously quantifying cytokine secretion, represents a potentially useful tool for COVID-19 therapeutics as well as for other emerging infectious diseases.

## Acknowledgements

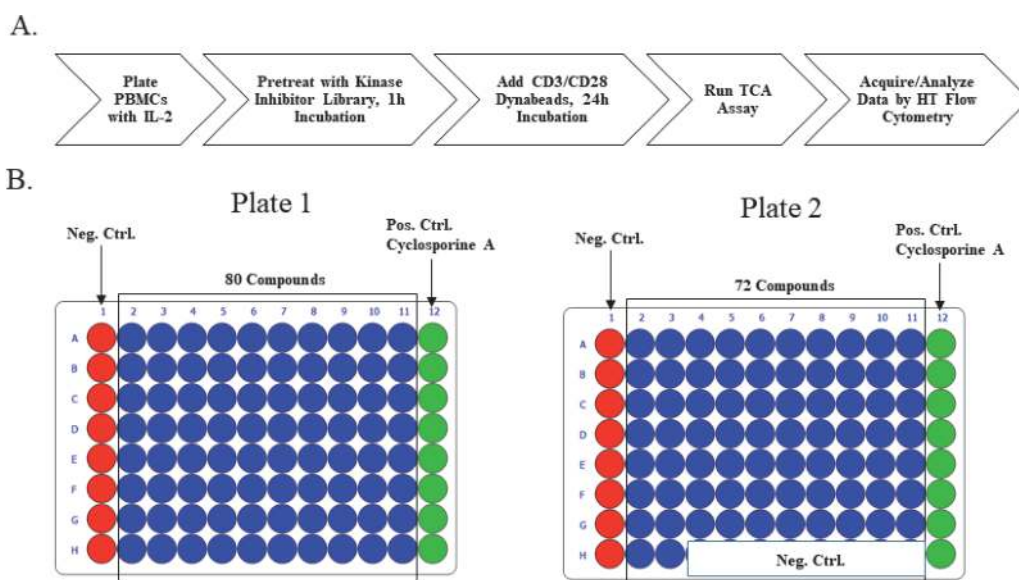
We thank all the members of the biology team at Sartorius iQue® for providing comments.

The authors received no financial support for the research, authorship, and/or publication of this article.

## Conflict of interest

The authors declare no conflict of interest.

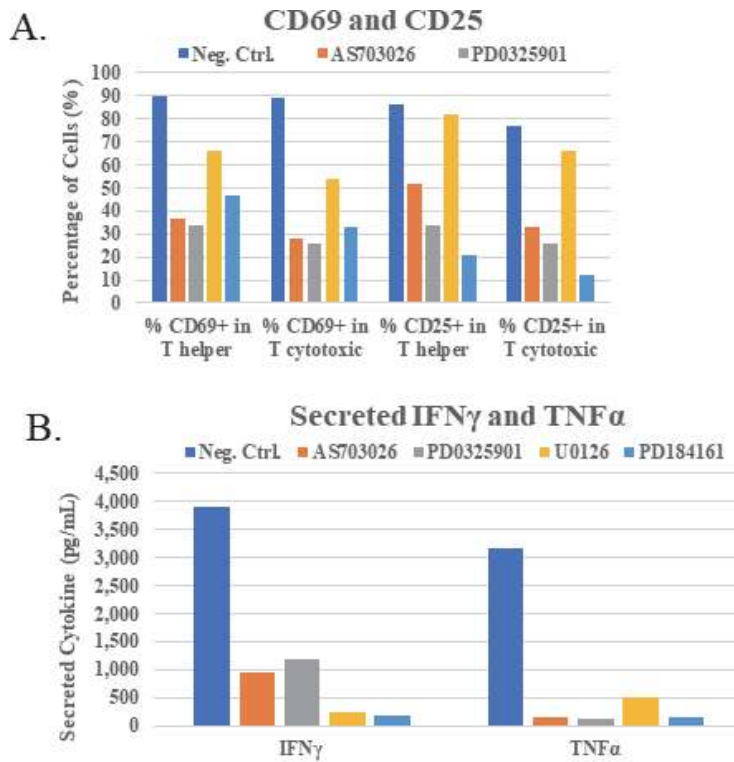
## Supplementary material



### Supplemental Figure 1.

The assay workflow and experimental plate layout for kinase inhibition screening. Supplemental Figure A shows the assay workflow beginning with plating cells, incubating cells with kinase inhibitor, cell activation, assay steps and high-throughput data acquisition. Supplemental Figure B shows the plate map layout showing negative controls in red, sample wells in blue and positive controls in green. The plate map for plate 2 follows the layout of plate one.





C.

	% CD69+ in T helper	% CD69+ in T cytotoxic	% CD25+ in T helper	% CD25+ in T cytotoxic	IFN $\gamma$	TNF $\alpha$
AS703026	0.008	0.011	0.010	0.019	0.019	0.006
PD0325901	0.012	0.031	0.015	0.017	0.017	0.002
U0126	0.990	3.364	1.237	0.773	0.773	0.314
PD184161	2.560	3.420	>10*	>10*	>10*	0.072

**Supplemental Figure 2.**

Four MEK1/2 inhibitors that inhibit relevant markers. The screening results showed that all 4 compounds broadly inhibit the major relevant markers (CD69 and CD25 expression, and IFN $\gamma$  and TNF $\alpha$  secretion) after 24-hour T cell activation. Supplement Figure 2A represents the inhibitory effect of MEK1/2 inhibitors on the expression of CD69 and CD25 on both T helper and T cytotoxic cells. Supplement Figure 2B illustrates the decreasing effects on the secretion of the cytokines IFN $\gamma$  and TNF $\alpha$ . In the subsequent dosage test to confirm the screening results (Supplement Figure 2C), 24 IC<sub>50</sub>s were generated from 4 compounds and 6 endpoints.

**Appendices and nomenclature**

- CAR-T      chimeric antigen receptor T cell
- TIL        tumor-infiltrating lymphocyte
- TCA        assay iQue® Human T Cell Activation Kit assay
- ACT        adoptive T cell transfer
- MHC       major histocompatibility complex


## **Author details**

Zhaoping Liu\*, Andrea Gomez-Donart, Caroline Weldon, Nina Senutovitch  
and John O'Rourke  
iQue® Sartorius, Albuquerque, NM, USA

\*Address all correspondence to: [zhaoping.liu@Sartorius.com](mailto:zhaoping.liu@Sartorius.com)

## **IntechOpen**

---

© 2021 The Author(s). Licensee IntechOpen. This chapter is distributed under the terms of the Creative Commons Attribution License (<http://creativecommons.org/licenses/by/3.0>), which permits unrestricted use, distribution, and reproduction in any medium, provided the original work is properly cited. 

## References

- [1] Medicines in Development for Autoimmune Diseases. *Pharmaceutical Research and Manufacturers of America* (PhRMA) 2016.
- [2] Tang J, Pearce L, Odonnell-Tormey J, Hubbard-Lucey VM. Trends in the Global Immuno-Oncology Landscape. *Nat. Rev. Drug Discov.* 2018;17:912–922. DOI: 10.1038/nrd.2018.167
- [3] Hosokawa K, Muranski P, Feng X, Townsley DM, Liu B, Knickelbein J, Keyvanfar K, Dumitriu B, Ito S, Kajigaya S, Taylor JG 6th, Kaplan MJ, Nussenblatt RB, Barrett AJ, O'Shea J, Young NS. Memory Stem T Cells in Autoimmune Disease: High Frequency of Circulating CD8+ Memory Stem Cells in Acquired Aplastic Anemia. *J Immunol.* 2016 Feb 15;196(4):1568–78. DOI: 10.4049/jimmunol.1501739
- [4] Schmidt RE, Grimbacher B, Witte T. Autoimmunity and primary immunodeficiency: two sides of the same coin? *Nat Rev Rheumatol.* 2017 Dec 19;14(1):7–18. DOI: 10.1038/nrrheum.2017.198
- [5] Raphael I, Nalawade S, Eagar TN, Forsthuber TG. T cell subsets and their signature cytokines in autoimmune and inflammatory diseases. *Cytokine.* 2015 Jul;74(1):5–17. DOI: 10.1016/j.cyto.2014.09.011
- [6] Sharma P, Allison JP. The future of immune checkpoint therapy. *Science.* 2015 Apr 3;348(6230):56–61. DOI: 10.1126/science.aaa8172
- [7] Thakur A, Huang M, Lum LG. Bispecific antibody based therapeutics: Strengths and challenges. *Blood Rev.* 2018 Jul;32(4):339–347. DOI: 10.1016/j.blre.2018.02.004
- [8] Zacharakis N, Chinnasamy H, Black M, Xu H, Lu YC, Zheng Z, Pasetto A, Langhan M, Shelton T, Prickett T, Gartner J, Jia L, Trebska-McGowan K, Somerville RP, Robbins PF, Rosenberg SA, Goff SL, Feldman SA. Immune recognition of somatic mutations leading to complete durable regression in metastatic breast cancer. *Nat Med.* 2018 Jun;24(6):724–730. DOI: 10.1038/s41591-018-0040-8
- [9] June CH, O'Connor RS, Kawalekar OU, Ghassemi S, Milone MC. CAR T cell immunotherapy for human cancer. *Science.* 2018 Mar 23;359(6382):1361–1365. DOI: 10.1126/science.aar6711
- [10] Almåsbak H, Aarvak T, Vemuri MC. CAR T Cell Therapy: A Game Changer in Cancer Treatment. *J Immunol Res.* 2016;2016:5474602. DOI: 10.1155/2016/5474602
- [11] Antonia SJ, Larkin J, Ascierto PA. Immuno-oncology combinations: a review of clinical experience and future prospects. *Clin Cancer Res.* 2014 Dec 15;20(24):6258–68. DOI: 10.1158/1078-0432.CCR-14-1457
- [12] Navarro MN, Cantrell DA. Serine-threonine kinases in TCR signaling. *Nat Immunol.* 2014 Sep;15(9):808–14. DOI: 10.1038/ni.2941
- [13] Ferguson FM, Gray NS. Kinase inhibitors: the road ahead. *Nat Rev Drug Discov.* 2018 May;17(5):353–377. DOI: 10.1038/nrd.2018.21
- [14] Frémin C, Meloche S. From basic research to clinical development of MEK1/2 inhibitors for cancer therapy. *J Hematol Oncol.* 2010 Feb 11;3:8. DOI: 10.1186/1756-8722-3-8
- [15] Bhullar KS, Lagarón NO, McGowan EM, Parmar I, Jha A, Hubbard BP, Rupasinghe HPV. Kinase-targeted cancer therapies: progress, challenges and future directions. *Mol Cancer.* 2018 Feb 19;17(1):48. DOI: 10.1186/s12943-018-0804-2

- [16] Gross S, Rahal R, Stransky N, Lengauer C, Hoefflich KP. Targeting cancer with kinase inhibitors. *J Clin Invest*. 2015 May;125(5):1780–9. DOI: 10.1172/JCI76094
- [17] Carnevalli LS, Sinclair C, Taylor MA, Gutierrez PM, Langdon S, Coenen-Stass AML, Mooney L, Hughes A, Jarvis L, Staniszevska A, Crafter C, Sidders B, Hardaker E, Hudson K, Barry ST. PI3K $\alpha/\delta$  inhibition promotes anti-tumor immunity through direct enhancement of effector CD8<sup>+</sup> T-cell activity. *J Immunother Cancer*. 2018 Dec 27;6(1):158. DOI: 10.1186/s40425-018-0457-0
- [18] Abril-Rodriguez, G., Torrejon, D.Y., Liu, W. *et al.* PAK4 inhibition improves PD-1 blockade immunotherapy. *Nat Cancer* 1, 46–58 (2020). DOI.org/10.1038/s43018-019-0003-0
- [19] Ding M, Kaspersson K, Murray D, Bardelle C. High-throughput flow cytometry for drug discovery: principles, applications, and case studies. *Drug Discov Today*. 2017 Dec; 22(12):1844–1850. DOI: 10.1016/j.drudis.2017.09.005
- [20] Sklar LA, Carter MB, Edwards BS. Flow cytometry for drug discovery, receptor pharmacology and high-throughput screening. *Curr Opin Pharmacol*. 2007 Oct;7(5):527–34. DOI: 10.1016/j.coph.2007.06.006
- [21] Yi JS, Cox MA, Zajac AJ. T-cell exhaustion: characteristics, causes and conversion. *Immunology*. 2010 Apr;129(4):474–81. DOI: 10.1111/j.1365-2567.2010.03255
- [22] Martinez EM, Klebanoff SD, Secrest S, Romain G, Haile ST, Emtage PCR, Gilbert AE. High-Throughput Flow Cytometric Method for the Simultaneous Measurement of CAR-T Cell Characterization and Cytotoxicity against Solid Tumor Cell Lines. *SLAS Discov*. 2018 Aug;23(7): 603–612. DOI: 10.1177/2472555218768745
- [23] Chen EW, Brzostek J, Gascoigne NRJ, Rybakin V. Development of a screening strategy for new modulators of T cell receptor signaling and T cell activation. *Sci Rep*. 2018 Jul 3;8(1):10046. DOI: 10.1038/s41598-018-28106-5
- [24] Knapp S. New opportunities for kinase drug repurposing and target discovery. *Br J Cancer*. 2018 Apr;118(7): 936–937. DOI: 10.1038/s41416-018-0045-6
- [25] Saibil SD, Ohashi PS. Targeting T cell activation in immuno-oncology. *Curr Oncol*. 2020 Apr;27(Suppl 2): S98-S105. doi: 10.3747/co.27.5285. Epub 2020 Apr 1. PMID: 32368179; PMCID: PMC7193998.
- [26] Sharma P, Hu-Lieskovan S, Wargo JA, Ribas A. Primary, Adaptive, and Acquired Resistance to Cancer Immunotherapy. *Cell* 2017 Feb 9;168(4):707–723. doi: 10.106/j.cell.2017.01.017. PMID: 28187290; PMCID: PMC5391692.
- [27] Wang Y, Zhang K, Georgiev P, Wells S, Xu H, Lacey BM, Xu Z, Laskey J, Mcleod R, Methot JL, Bittinger M, Pasternak A, Ranganth S. Pharmacological inhibition of hematopoietic progenitor kinase 1 positively regulates T-cell function. *PLoS One*. 2020 Dec 3;15(12):e0243145. doi: 10.1371/journal.pone.0243145. PMID: 33270695; PMCID: PMC7714195.
- [28] Zheng HY, Xu M, Yang CX, Tian RR, Zhang M, Li JJ, Wang XC, Ding ZL, Li GM, Li XL, He YQ, Dong XQ, Yao YG, Zheng YT. Longitudinal transcriptome analyses show robust T cell immunity during recovery from COVID-19. *Signal Transduct Target Ther*. 2020 Dec 24;5(1):294. doi: 10.1038/s41392-020-00457-4. PMID: 33361761; PMCID:PMC7758413.

[29] Kuri-Cervantes L, Pampena MB, Meng W, Rosenfeld AM, Ittner CAG, Weisman AR, Agyekum RS, Mathew D, Baxter AE, Vella LA, Kuthuru O, Apostolidis SA, Bershaw L, Dougherty J, Greenplate AR, Pattekar A, Kim J, Han N, Gouma S, Weirick ME, Arevalo CP, Bolton MJ, Goodwin EC, Anderson EM, Hensley SE, Jones TK, Mangalmurti NS, Luning Prak ET, Wherry EJ, Meyer NJ, Betts MR. Comprehensive mapping of immune perturbations associated with severe COVID-19. *Sci Immunol.* 2020 Jul 15;5(49):eabd7114. doi: 10.1126/sciimmunol.abd7114. PMID:32669287; PMCID: PMC7402634.